

Magnetic dipole rotational bands in odd-*A* Rb isotopes

Amita and A. K. Jain

*Department of Physics, University of Roorkee, Roorkee - 247 667, India*

V. I. Dimitrov\* and S. G. Frauendorf†

*Department of Physics, University of Notre Dame, Notre Dame, Indiana 46556*

(Received 28 February 2001; published 16 August 2001)

The hybrid version of tilted axis cranking has been used to study the existence of magnetic rotation in the  $\Delta I=1$  bands of odd-*A*  $^{79,81,83,85}\text{Rb}$  isotopes. The bands are found to be built on prolate three quasiparticle  $\pi(g_{9/2}) \otimes \nu[g_{9/2}(fp)^1]$  configuration. The results exhibit a rapid onset and decline of magnetic rotation as we go from  $N=42$  to 48. The  $^{83}\text{Rb}$  appears to be a better case of magnetic rotation among these four Rb isotopes.

DOI: 10.1103/PhysRevC.64.034308

PACS number(s): 21.60.-n, 21.10.-k, 27.50.+e

## INTRODUCTION

The observation of rotational bands is usually associated with a nonsphericity in nuclei. The energy levels of these bands are quite regular and generally connected by electric quadrupole ( $E2$ ) transitions. It was therefore surprising that quasirotational bands were observed to be associated with configurations which are known to be nearly spherical. First observation of such rotational bands was made by Hübel *et al.* [1] and Clark *et al.* [2] in 1992, who observed regular patterns of gamma rays in the spectra of  $^{198,199}\text{Pb}$  nuclei. A further peculiarity was that the intraband transitions were not of  $E2$  type but  $M1$  (magnetic dipole) in nature. These bands have now been termed as “magnetic dipole” or “magnetic rotational” bands [3]. Since the existence of an anisotropic charge density in nuclei results in a breaking of the spherical symmetry which leads to the observation of rotational motion, it is clear that some kind of anisotropy is also playing an important role in the formation of magnetic rotational bands. The “shears mechanism” proposed by S. Frauendorf does provide for the breaking up of spherical symmetry even in nearly spherical nuclei. The anisotropy now exists in currents and hence the magnetic dipoles, which rotate about a tilted axis [4].

A recent compilation of the most likely candidates of magnetic rotation (MR) bands [5] lists as many as 120 MR bands observed in 56 nuclei spread over four mass regions namely  $A=80$  ( $Z=35-37$ ),  $110$  ( $Z=48-51$ ),  $135$  ( $Z=54-64$ ), and  $195$  ( $Z=80-86$ ). The largest number of bands are observed in the  $A \approx 195$  mass region where 12 lead isotopes having  $191 \leq A \leq 202$  display 42 MR bands. The theoretical calculations are also highly supportive of the shears mechanism interpretation of the MR in the lead region. Most of these calculations are based on the tilted axis cranking (TAC) model [3]. The cranking model assumes that the rotation takes place about one of the principal axes of the nuclear matter density distribution. However, the possibility

of rotation about any other axis also exists and this leads to the tilted axis generalization of the cranking model. While sufficient experimental and theoretical evidence exists for MR phenomena in the  $A=190$  and  $A=110$  mass regions, the evidence is lacking in other mass regions. This is particularly true for the  $A=80$  mass region where both the theoretical as well as experimental evidence is small.

The MR bands in the  $A=190$  and  $A=110$  mass regions are found to display some common features: (i) They are  $\Delta I=1$  ( $M1$ ) structures with  $B(M1)$  values of the order of several Weisskopf units. (ii) Crossover  $\Delta I=2$  ( $E2$ ) are either absent or very weak indicative of small deformation, enhancing the ratio  $B(M1)/B(E2)$  to  $\sim 10-100(\mu_N/eb)^2$ . (iii) The bandhead lies at a high excitation energy (a few MeV) and has a high spin ( $I \sim 10-15\hbar$ ) indicative of a multiquasiparticle character. (iv) The most important signature of a MR band as suggested by shears mechanism is a sharp decrease in the  $B(M1)$  values with increasing angular momentum.

In 1995, Tabor and Döring [6] listed a group of bands in the  $A=80$  region, whose properties were similar to the  $\Delta I=1$  bands seen in other mass regions. First confirmation for the MR in  $A=80$  mass region came in 1999, when two odd-odd isotopes of Rb were shown to carry the characteristic signature of decreasing  $B(M1)$  values with increasing spin for one band each in  $^{82,84}\text{Rb}$  [7-9]. Our compilation [5] lists six Rb isotopes as possibly containing one MR band each. More specifically,  $^{79,81,83,85}\text{Rb}$  (odd- $Z$ , odd- $A$ ) and  $^{82,84}\text{Rb}$  (odd-odd) isotopes are found to have a band each at an excitation energy  $\geq 2.0$  MeV and a bandhead spin  $\geq 6.5\hbar$ . The levels of these negative parity bands are connected by strong  $\Delta I=1$  transitions with very weak or absent crossover  $E2$  transitions. Most of the experimental data except  $^{82,83,84}\text{Rb}$  were obtained prior to 1995 and these bands were not looked upon as cases of MR phenomenon.

The aim of the present paper is twofold. First, we want to study the existence of MR in the odd- $A$  Rb isotopes. Second, we want to test the applicability of the recently introduced “hybrid version” of the TAC model [10] in the  $A=80$  mass region. The hybrid version of the TAC was recently introduced to remove the discrepancies between theoretical calculations and experimental data in the case of the four quasiparticle MR band in  $^{128}\text{Ba}$ . A study of series of Rb isotopes is also expected to shed light on the evolution of the shears

\*On leave of absence from Faculty of Physics, Sofia University, BG-1164 Sofia, Bulgaria.

†Also at Research Center Rossendorf, D-01314 Dresden, Germany.

mechanism as we move away from the  $N=50$  closed shell. The results of our calculations suggest a rapid development of magnetic rotation and its rapid dissolution occurs in odd- $A$  Rb isotopes. An experimental study of these isotopes is therefore most desirable.

### THE HYBRID TAC

The TAC model based on the Nilsson model potential [11] was based on the standard set of parameters [12]. This parameter set, however, does not work well in the  $A=130$  region and optimized set of parameters was suggested in Ref. [13]. The hybrid model proposed by Dimitrov, Dönau, and Frauendorf [10], tries to overcome the difficulty by making use of the best of the Woods-Saxon and Nilsson models and combine them. Thus the single particle energies of the spherical Woods-Saxon are taken and combined with the deformed part of the anisotropic harmonic oscillator. This approximation carries the advantage of using a realistic flat bottom potential along with the coupling between the oscillator shells taken into account in a simple way. A detailed account of the TAC may be found in Ref. [14] and the hybrid version in Ref. [10]. Here we present a brief account.

The mean field Hamiltonian of a rotating field for either neutrons or protons, is written as

$$h' = h_{sp} - \Delta(P^+ + P) - \lambda n - \omega(j_1 \sin \theta \cos \phi + j_2 \sin \theta \sin \phi + j_3 \cos \theta). \quad (1)$$

Here  $h_{sp}$  is the single particle Hamiltonian in a deformed field consisting of  $h_{sp} = h_{sph} + V_{def}$ . The spherical part,  $h_{sph}$ , is taken from the spherical Woods-Saxon potential with universal parameters [15]. The deformed potential  $V_{def}$  is taken from the Nilsson deformed potential [12]. The monopole pairing operator  $P = \sum C_K C_{\bar{K}}$  together with the gap parameter  $\Delta$  determines the pairing field. We have chosen  $\Delta$  as 80% of the odd-even mass difference  $\Delta_{oe}$  for protons and neutrons, calculated using the expressions given in Ref. [16] with the binding energies taken from the atomic mass table [17]. The chemical potential  $\lambda$  is fixed to reproduce the correct particle number.

We carry out planar TAC calculations by keeping  $\phi = 0^\circ$ . If we also put  $\theta = 0^\circ$  or  $90^\circ$ , the standard cranking model may be recovered. The angle  $\theta$  decides the tilt of the cranking axis with respect to the  $z$  axis in the  $x$ - $z$  plane of the intrinsic frame of reference.

The total Routhian  $E(\omega)$  is calculated by using the Strutinsky renormalization technique [18],

$$E(\omega) = E_{LD} - E_{smooth} + \langle \omega | h' | \omega \rangle. \quad (2)$$

Here,  $E_{LD}$  is the liquid drop energy and the smooth part of energy  $E_{smooth}$  is calculated by the Strutinsky averaging method. The equilibrium angle  $\theta$  is calculated by using the condition that the expectation values of the total angular momentum and the angular velocity are parallel. This gives

$$\tan \theta = \frac{\omega_1}{\omega_3} = \frac{J_1}{J_3}, \quad (3)$$

where  $J_1$  and  $J_3$  are the components of total angular momentum  $\vec{J}$  along the 1 and 3 axis, respectively.

The total Routhian (2) is then minimized with respect to the deformation parameters ( $\epsilon_2, \gamma$ ) to obtain the minimum for a chosen configuration and a cranking frequency  $\omega$ . We then fix the deformation parameters at these values and calculate the total energy for each  $\omega$  at the corresponding equilibrium angle  $\theta$ . To compare the experimental results with the calculated ones, we transform the experimental energies  $E(I)$  into the rotational frequencies by using the relation

$$\hbar \omega(I) = E(I) - E(I-1). \quad (4)$$

### ELECTROMAGNETIC TRANSITION STRENGTHS

Shears mechanism suggests the almost perpendicular coupling of neutron and proton angular momenta at the bandhead gives rise to a large perpendicular component of magnetic moment  $\mu_\perp = \mu_\perp \pi + \mu_\perp \nu$ . The total angular momentum along the band increases by tilting the proton and neutron blades towards it thereby decreasing  $\mu_\perp$ . A decreasing trend of the  $B(M1)$  values is therefore a natural consequence of the shears mechanism.

From the semiclassical expressions, the reduced transition probabilities are given by [14]

$$B(M1, \Delta I = 1) = \frac{3}{8\pi} (\mu_\perp)^2 = \frac{3}{8\pi} (\mu_3 \sin \theta - \mu_1 \cos \theta)^2 \quad (5)$$

and

$$B(E2, \Delta I = 2) = \frac{15}{128\pi} \left[ Q'_0 \sin^2 \theta + \sqrt{\frac{2}{3}} Q'_2 (1 + \cos^2 \theta) \right]^2. \quad (6)$$

Here,  $\mu$ 's are the expectation values of the corresponding operator of the magnetic moment and  $Q$ 's are the expectation values of the intrinsic quadrupole moment operator. The expectation values of the proton and neutron spins are attenuated by a factor of 0.7 for the calculation of  $B(M1)$  values.

### RESULTS AND DISCUSSION

Since the spins of the observed bands are high ( $\geq 5.5\hbar$ ), the configuration may involve both high- $j$  proton and neutron orbitals which is also necessary for the occurrence of the shears mechanism. Since the odd- $A$  Rb isotopes are odd- $Z$ , even- $N$  systems, the configuration should consist of odd number of quasiprotons and an even number of quasineutrons. The active high- $j$  orbital close to the Fermi level for both protons and neutrons in Rb isotopes is the positive parity  $g_{9/2}$  orbital. Since the bands have a negative parity, we also need a negative parity orbital. The negative parity orbital close to the Fermi level is the mixed ( $f_{5/2} p_{1/2}$ ) orbital having  $N=3$ . The lowest lying negative parity three quasiparticle configuration in the case of odd- $A$  <sup>79,81,83,85</sup>Rb isotopes, which gives rise to a shears mechanism, comes out to be  $\pi(g_{9/2}) \otimes \nu[g_{9/2}(fp)^1]$ . We have therefore chosen this configuration for our calculations. Since pairing is an important parameter in these calculations, we have done all the

TABLE I. Calculated values of deformation parameters corresponding to the pairing gap parameters from the mass data, and constant pairing.

A	$\Delta_p$	$\Delta_n$	$\epsilon_2$	$\gamma$	For $\Delta_p = \Delta_n = 0.8$	
					$\epsilon_2$	$\gamma$
79	1.42	0.89	0.17	15	0.17	-10
81	1.45	0.89	0.17	10	0.17	10
83	1.44	0.87	0.17	10	0.17	10
85	1.26	0.71	0.17	-20	0.17	10

calculations for two sets of pairing parameters, one with the calculated values of  $\Delta_p$  and  $\Delta_n$  obtained by using the mass data as described in the previous section and second, keeping these parameters fixed at 0.8 MeV for both protons and neutrons. For two-quasineutrons in the configuration, one would expect more reduction of the neutron pairing gap parameter. To check the effect of reduced pairing, we have performed a test calculation for  $^{83}\text{Rb}$  taking  $\Delta_n = 0.1$ . We find that the results remain nearly same. We have therefore performed all the calculations with a neutron pairing gap as 80% of the odd-even mass difference. The value of  $\omega$  for calculating the deformation parameters, has been chosen to be close to the lowest  $\gamma$  ray of corresponding band and therefore the deformation parameters in our calculations have been calculated at  $\omega = 0.3, 0.15, 0.15$ , and  $0.5$  for  $^{79,81,83,85}\text{Rb}$ , respectively. The values of the calculated pairing gap parameters  $\Delta_p$ ,  $\Delta_n$  and the corresponding deformation parameters  $\epsilon_2$  and  $\gamma$  along with the values of deformation parameters for fixed

$\Delta_p = \Delta_n = 0.8$  MeV for each of the four Rb isotopes are given in Table I. It is seen that the pairing gap affects the triaxial deformation parameter  $\gamma$ .

In the following discussion, the experimental data for  $^{79,81,83,85}\text{Rb}$  are taken from Ref. [5]. Reference [9] reports two  $M1$  bands in  $^{83}\text{Rb}$ , namely band C and band D. Both these bands are quite irregular in energies. Also, band C does not exhibit a decreasing pattern of  $B(M1)$  values; the authors [9] therefore conclude that this band is not a shears band. The data on band D is not sufficient to make any meaningful conclusion. However, a more intense band on top of the 2067-keV level is quite regular and this is the band reported by Amita *et al.* [5] as a possible candidate for magnetic rotation. Henceforth we compare this band with the theoretical results in the following discussion.

The results of our calculations are shown in Fig. 1 where we plot the experimental and calculated level energies as a function of total angular momentum. The zero point of the energies is arbitrary. The calculations are able to reproduce the slopes of the curves in all the cases except the dashed curve in  $^{79}\text{Rb}$ . This in a way supports the configuration assignment as  $\pi(g_{9/2}) \otimes \nu[g_{9/2}(fp)^1]$ . The effect of pairing gap parameter can also be seen in the results plotted for a constant pairing  $\Delta_p = \Delta_n = 0.8$  MeV (dashed line). The effect of pairing shows up more clearly in Fig. 2, where we plot the total angular momentum  $I$  as a function of rotational frequency  $\hbar\omega$  in units of MeV. It is clear from the plots that the results are quite sensitive with respect to the pairing gap parameters  $\Delta_p$  and  $\Delta_n$  and the ones corresponding to the pairing gap parameters estimated from mass data come closer to the experimental data. The reduced value of the

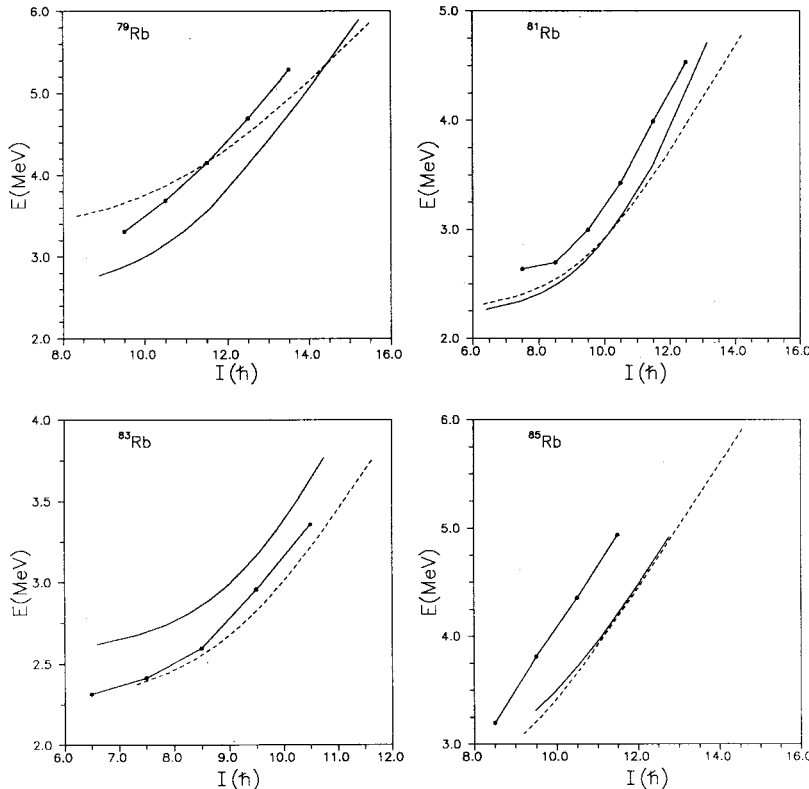


FIG. 1. Level energies  $E$  vs the total angular momentum  $I$  for  $^{79,81,83,85}\text{Rb}$ . Full circles in all the figures represent the experimental data taken from Ref. [5] and the references cited therein. Solid lines are the results with the calculated  $\Delta_p$  and  $\Delta_n$  values obtained from the mass data whereas the dashed lines are for a constant pairing  $\Delta_p = \Delta_n = 0.8$  MeV.

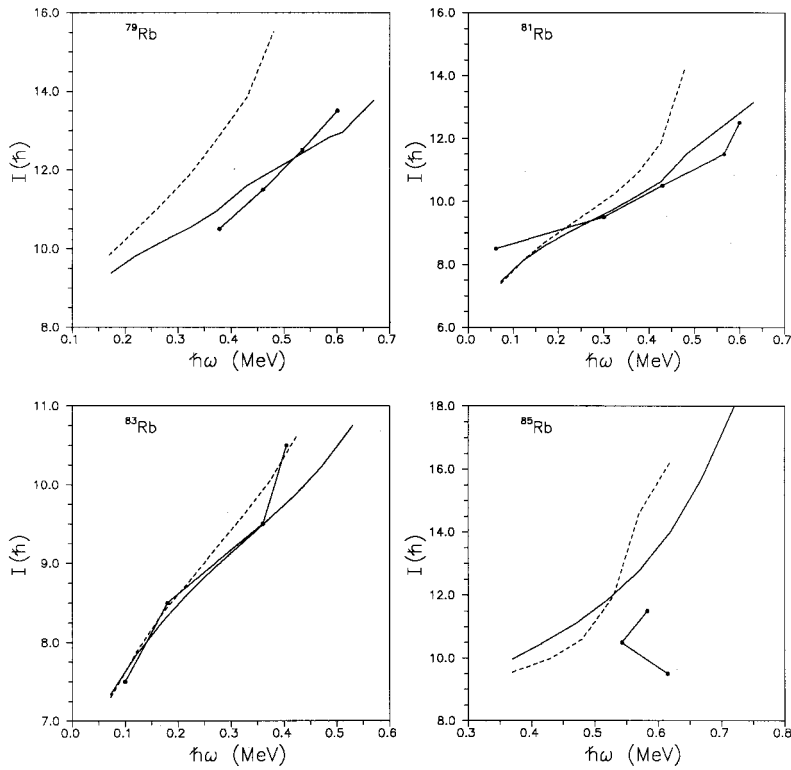


FIG. 2. Total angular momentum  $I$  vs the rotational frequencies ( $\hbar\omega$ ). Description of lines is the same as given in Fig. 1.

neutron pairing gap parameter  $\Delta_n$  is close to 0.8 MeV, whereas the proton pairing gap parameter  $\Delta_p$  is nearly 1.2 MeV for all the cases.

As already pointed out, the variation of  $B(M1)$  values as

a function of the total angular momentum  $I$  is a critical test of magnetic rotation. No experimental data are available for the electromagnetic transition probabilities of these four isotopes of Rb. To see the existence of MR in odd- $A$  Rb iso-

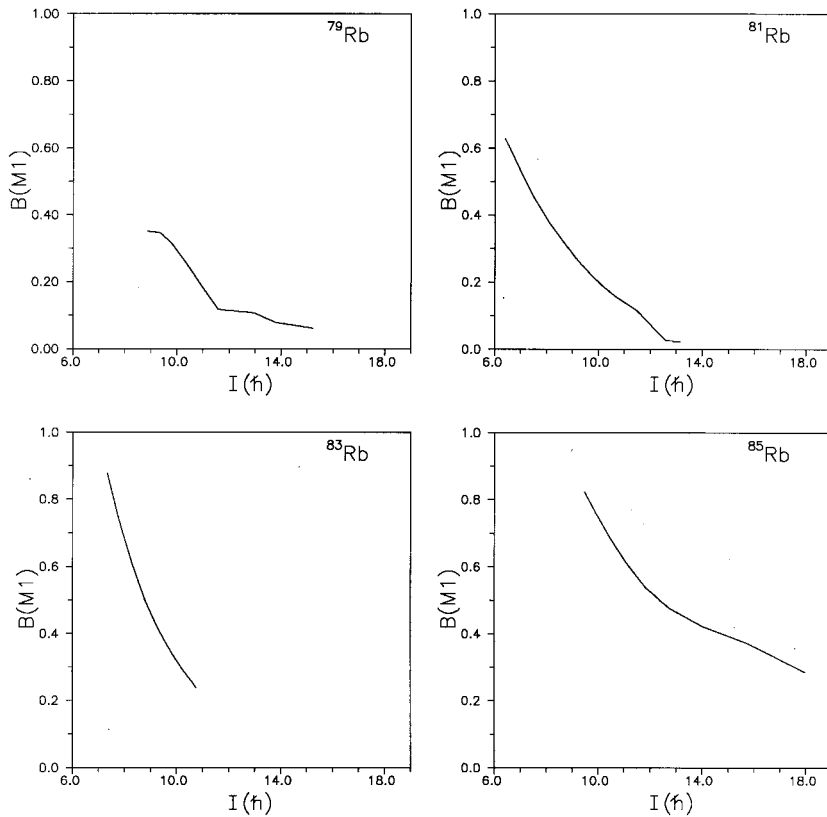


FIG. 3.  $B(M1)(\mu_N)^2$  vs  $I$ . The pairing gap parameters  $\Delta_p$  and  $\Delta_n$  are obtained from the mass data.

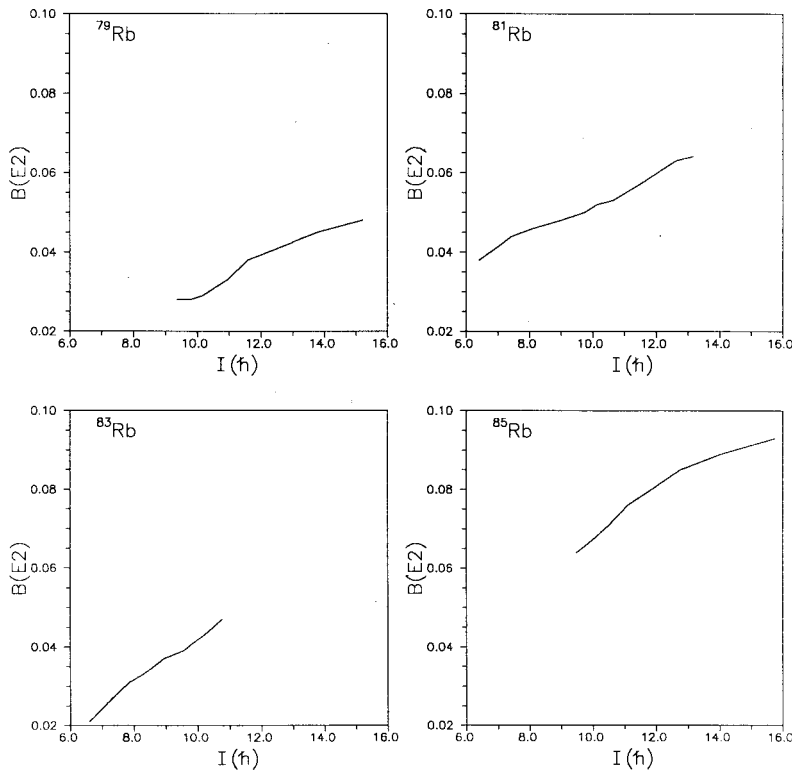


FIG. 4.  $B(E2)(eb)^2$  vs  $I$ . The pairing gap parameters  $\Delta_p$  and  $\Delta_n$  are obtained from the mass data.

topes, we plot the  $B(M1)$  values vs the total angular momentum  $I$  in Fig. 3. We find that the  $B(M1)$  values indeed decrease with rise in the angular momentum in all the cases indicating the presence of magnetic rotation in these odd-A Rb isotopes. A closer look at the plots clearly shows that the fall in the  $B(M1)$  values is greatest in the case of  $^{83}\text{Rb}$  ( $N$

$=46$ ). Considering all the features, it appears to be the best case for magnetic rotation among the four Rb isotopes. This is in line with the reported observation of magnetic rotation in  $^{82,84}\text{Rb}$  which lie on either side of  $^{83}\text{Rb}$ .

This conclusion is further supported by plots of  $B(E2)$  values vs  $I$  (Fig. 4) and also the ratios  $B(M1)/B(E2)$  vs  $I$

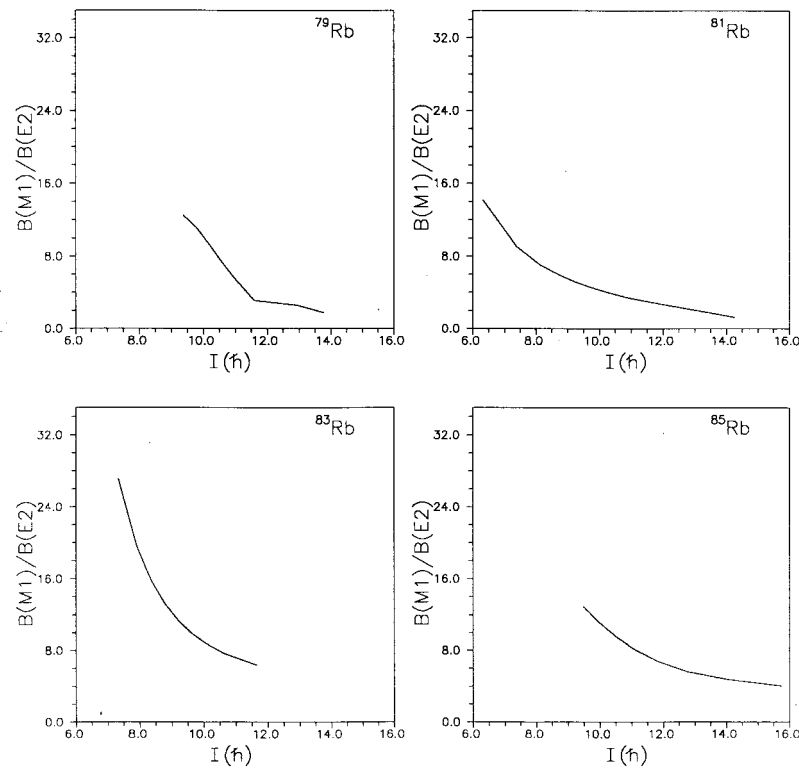


FIG. 5.  $B(M1)/B(E2)(\mu_N/eb)^2$  vs  $I$ . The pairing gap parameters  $\Delta_p$  and  $\Delta_n$  are obtained from the mass data.

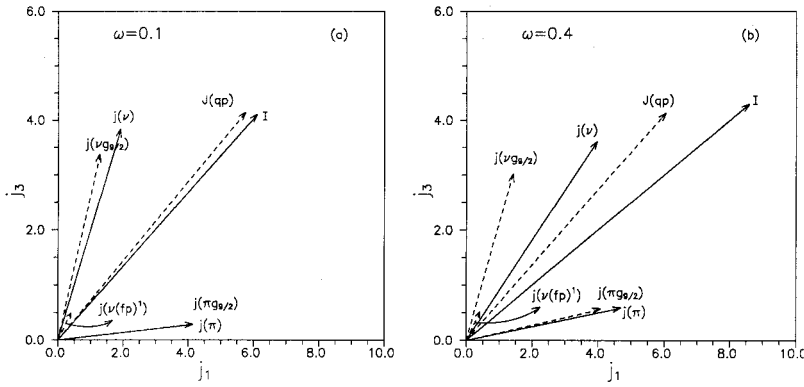


FIG. 6. The angular momentum coupling scheme for  $^{83}\text{Rb}$  for both the quasiparticle angular momenta (dashed lines) and the total angular momenta (solid lines).

(Fig. 5). We find that the  $B(E2)$ 's are lowest (between approximately 3 and 7 W.u.) in the case of  $^{83}\text{Rb}$ ; the  $B(E2)$ 's rise on either side of the  $^{83}\text{Rb}$  isotope. Also, the  $B(E2)$  values are very small in magnitude indicating that the intra-band transitions are predominantly  $M1$  in nature. This also shows up in Fig. 5 where we note a large  $B(M1)/B(E2)$ , decreasing sharply with rise in angular momentum along the band in  $^{83}\text{Rb}$ . A comparison with the experimental  $B(M1)/B(E2)$  ratios could not be made due to the lack of data on  $\gamma$  ray branching ratios and mixing ratios. In Ref. [6], the authors present lower limits on the  $B(M1)/B(E2)$  ratios in  $^{79}\text{Rb}$  of two lowest  $\gamma$  ray transitions which are close to  $10(\mu_N/eb)^2$ ; the calculated values are quite close to these values.

The angular momentum coupling scheme for  $^{83}\text{Rb}$  is shown in Fig. 6. Here we see that the total angular momentum is generated by the quasiparticle contribution only at lower rotational frequency ( $\omega=0.1$ ). However, the situation changes at high rotational frequency ( $\omega=0.4$ ) where the effect of rotation on the total angular momentum is directly visible. Since the deformation is larger ( $\epsilon_2=0.17$ ) than what we generally expect for a pure magnetic rotation ( $\epsilon_2 < 0.15$ ), there is a finite rotational contribution to the total angular momentum. The proton and neutron angular momentum blades exhibit a definite closing towards the total angular momentum as the rotational frequency rises. Due to the existence of a finite rotational angular momentum, we cannot label  $^{83}\text{Rb}$  as a pure magnetic rotor, but it certainly is a good case of magnetic rotation. We also note that in going from  $^{79}\text{Rb}$  to  $^{85}\text{Rb}$  as we approach the magic number  $N=50$ , we

observe a rapid development and decline of MR. Presence of deformation, however, does not seem to destroy the phenomenon. Such a rapid development of MR has not been seen so far in any other mass region. This makes the odd- $A$  Rb isotopes ideal for experimental work.

## CONCLUSIONS

To conclude, we may say that the shears mechanism holds good in the  $\Delta I=1$  bands of odd- $A$   $^{79,81,83,85}\text{Rb}$  isotopes, although it is not the only mechanism responsible for the generation of angular momentum. With a deformation of  $\epsilon_2=0.17$  the nuclides do not classify as pure magnetic rotors. They lie at the beginning of the transitional region between magnetic and conventional collective regions. The variation of  $B(M1)$  with angular momentum indicates a rapid onset and a decline in magnetic rotation as we move away from the magic number  $N=50$ . The  $B(E2)$  values and the  $B(M1)/B(E2)$  ratios also support this trend. The  $^{83}\text{Rb}$  isotope appears to be a better case of magnetic rotation among the four isotopes discussed here. Experimental confirmation of these results would be most interesting.

## ACKNOWLEDGMENTS

We are thankful to Dr. Balraj Singh for helpful discussions. We acknowledge financial support from the Department of Science and Technology (Government of India) and Council of Scientific and Industrial Research (Government of India). This work was also supported by the U.S. DOE Grant No. DE-FG02-95ER40934.

- [1] H. Hübel *et al.*, Prog. Part. Nucl. Phys. **28**, 427 (1992).
- [2] R. M. Clark *et al.*, Phys. Lett. B **275**, 247 (1992).
- [3] S. Frauendorf, Nucl. Phys. **A557**, 259c (1993).
- [4] S. Frauendorf, Rev. Mod. Phys. **73**, 463 (2001).
- [5] Amita, A. K. Jain, and B. Singh, At. Data Nucl. Data Tables **74**, 283 (2000).
- [6] S. L. Tabor and J. Döring, Phys. Scr. **T56**, 175 (1995).
- [7] J. Döring *et al.*, Phys. Rev. C **59**, 71 (1999).
- [8] H. Schnare *et al.*, Phys. Rev. Lett. **82**, 4408 (1999).
- [9] R. Schwengner *et al.*, J. Res. Natl. Inst. Stand. Technol. **105**, 133 (2000).
- [10] V. I. Dimitrov, F. Dönau, and S. Frauendorf, Phys. Rev. C **62**, 024315 (2000).
- [11] F. Dönau *et al.*, Nucl. Phys. **A584**, 241 (1995).
- [12] S. G. Nilsson *et al.*, Nucl. Phys. **A131**, 1 (1969).
- [13] Jing-ye Zhang *et al.*, Phys. Rev. C **39**, 714 (1989).
- [14] S. Frauendorf, Nucl. Phys. **A677**, 115 (2000).
- [15] R. Bengtsson *et al.*, Phys. Scr. **39**, 196 (1989).
- [16] R. Bengtsson, S. Frauendorf, and F. R. May, At. Data Nucl. Data Tables **35**, 15 (1986).
- [17] A. H. Wapstra and G. Audi, Nucl. Phys. **A595**, 409 (1995).
- [18] V. M. Strutinsky, Nucl. Phys. **A95**, 420 (1967).